

Determination of Horizontal Tail Load and Hinge Moment Characteristics from Flight Data

Gary D. Park* and Mike H. Ablat†
Gates Learjet Corporation, Wichita, Kansas

Horizontal tail load and hinge moment derivatives were obtained from flight data through the use of parameter identification techniques. For these analyses, strain gage data were used in conjunction with gyroscope, accelerometer, and other airplane response measurements. The resulting derivatives were compared with full- and small-scale wind-tunnel data. The strain gage measurements are shown to be a practical means of obtaining hinge moment derivatives and improving the accuracy of other derivatives.

Nomenclature

a_n	= normal acceleration at the center of gravity, g
ACTLOD	= load on the actuator, lb
FE, F_e	= pilot elevator control force, lb
g	= acceleration due to gravity, ft/s^2
G_e	= elevator gearing ratio, 1/in.
H_e	= elevator hinge moment, in.-lb
I_y	= moment of inertia about y -body axes, slug- ft^2
i_H	= horizontal stabilizer incidence angle, rad or deg
K_l	= downspring force when $i_H = 0$, lb
K_{i_H}	= variation of downspring force with i_H , lb/deg
l	= distance from airplane center of gravity to the center of pressure of the horizontal tail, ft
m	= W/g , slugs
M	= pitching moment/ I_y , rad/s^2
N	= normal force/ mV , 1/s
q	= pitch rate, rad/s or deg/s
\bar{q}	= dynamic pressure, lb/ft^2
S	= wing area, ft^2
V	= velocity, ft/s
W	= airplane gross weight, lb
α	= waterline angle of attack, rad or deg
δ_e	= elevator deflections, rad or deg
θ	= pitch angle, rad or deg
$\partial\epsilon/\partial\alpha$	= variation of downwash angle with angle of attack

Superscripts

(\cdot)	= the partial derivative of that parameter with respect to time
($-$)	= fixed value

Subscripts

H	= horizontal stabilizer
0	= initial
q, α, i_H, δ_e	= partial derivatives with respect to subscripted variables

Introduction

VERIFICATION of derivatives used in airload analyses during FAA certification of the Model 55 business jet airplane was accomplished using parameter identification computer programs developed at NASA. The computer program developed by Taylor and Iliff was used extensively.¹ However, some work was done using the newer, more elaborate program developed by Maine and Iliff.^{2,3} These programs were utilized because, in some form, they have been widely used in research and industry since 1968.⁴ These techniques have made analog computation for determining derivatives from flight data obsolescent and are at least rivaling the wind tunnel in both sophistication and data reliability. Although many available sources exist which explain the mathematical formulation of the parameter identification technique, Fig. 1 presents a simplified block diagram for illustration.¹⁻⁴

Past studies of similar business jet airplanes provided useful comparison data and methods. A full-scale wind-tunnel test of the model 23 in the NASA Ames 40 × 80 ft wind tunnel was conducted.⁵ These results were compared with small-scale wind-tunnel tests.⁶ Wingrove obtained in-flight derivatives using least-squares on a model 23.^{7,8} Strain gages mounted on a model 35 empennage permitted the determination of empennage and tail-off derivatives.⁹⁻¹¹ While evaluating translational acceleration derivatives from flight data, Maine and Iliff made estimates of downwash on the horizontal tail of a jet trainer using approximation techniques.¹² This study expands the utilization of parameter identification techniques to the determination of horizontal tail load and hinge moment derivatives from strain gage measurements.

The literature is abundant with comparisons of the various parameter identification techniques with wind-tunnel and analytical results.¹³⁻¹⁵ These comparisons include airplanes of all types.¹⁶⁻¹⁸ Many investigations have been performed to establish the merits of these techniques and include comparisons of various parameter estimation techniques, turbulence effects, magnitudes of parameter uncertainty, modeling errors, instrumentation errors, and more.¹⁹⁻²⁵ Expanded applications are being developed, and some because of improved instrumentation.^{19,26-30} Strain gage measurements also provide new applications such as presented and can improve the accuracy of other derivatives.^{2,19,25}

Test Airplane

The airplane used in these analyses was the model 55 shown in Fig. 2. The results of the analyses are compared with full-scale wind-tunnel tests of the model 23 shown in the

Presented as Paper 82-0183 at the AIAA 20th Aerospace Sciences Meeting, Orlando, Fla., Jan. 11-14, 1982; submitted Jan. 22, 1982; revision received Nov. 30, 1982. Copyright © American Institute of Aeronautics and Astronautics, Inc., 1982. All rights reserved.

*Group Engineer. Associate Fellow AIAA.

†Technical Director. Associate Fellow AIAA.

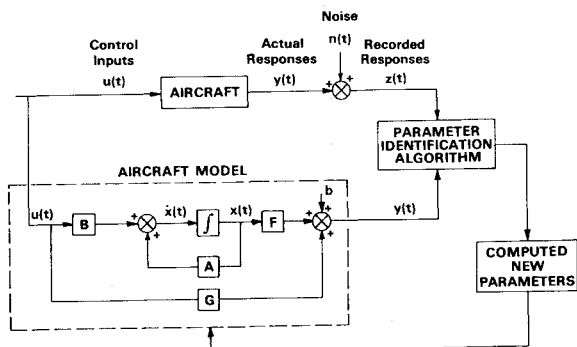


Fig. 1 Parameter identification technique.

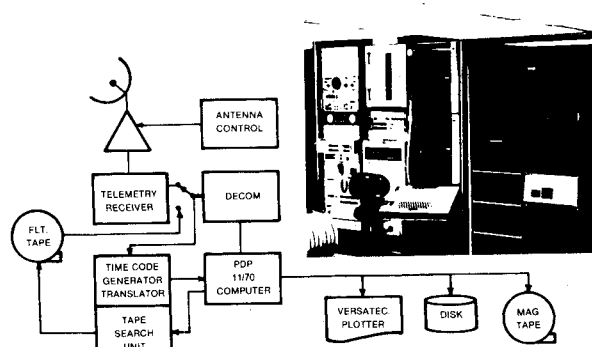


Fig. 3 Real-time data acquisition system.

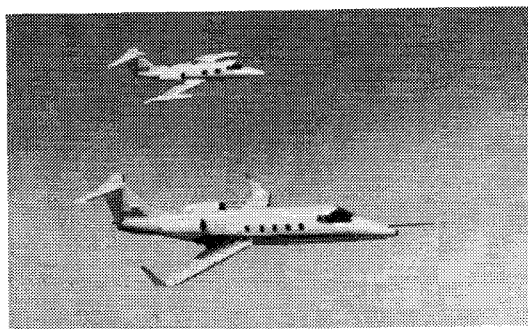


Fig. 2 Model 55 with model 23.

background of the photograph. Model 55 has a bigger fuselage which is larger in diameter, the vertical tail has an extension plug, the wing has been extended, and winglets replaced the tip tanks. The horizontal tails are nearly identical and the bullet-shaped fairing at the top of the vertical no longer exists. Also, TFE 731-3 turbofan engines are on the model 55, whereas, model 23 uses CJ610-4 turbojets.

Instrumentation and Data Reduction

The elevator hinge moment was determined from strain gages formed in a Wheatstone bridge mounted to a torque tube fixed along the hinge line to the inboard spar. The other end of the torque tube was mounted to the elevator bellcrank. Elevator stick forces produced by the pilot were obtained from a strain gage mounted on the pilot's control column. Airloads on the horizontal stabilizer were determined from a strain gage mounted on the actuator which rotates the stabilizer for trim. Thus, forces on the actuator (ACTLOD) were measured directly. The elevator deflections were measured using ceramic rheostats on the control surface. The airplane angle of attack was measured using a vane mounted on the nose boom shown in Fig. 2. The airplane pitch attitude and pitch rate were measured from gyroscopes, and normal acceleration was measured from an accelerometer.

The real-time data acquisition system shown in Fig. 3 consists of an antenna controller, a telemetry receiver, a PCM decom, a time code generator/translator, and tape search unit. The 256K byte computer uses magnetic tape, two disk drives, a printer/plotter, and a graphics terminal.³¹

Longitudinal Control System

The horizontal stabilizer is shown in Fig. 4. It is an all-movable stabilizer that rotates about a pin as shown. The actuator is a screw jack operated by an electric motor.

The elevator control system is shown in Fig. 5. The pilot control column attaches to cables that operate a sector which causes the push rod to move. The push rod splits into a "Y" to connect to the two bellcranks. The downspring assembly attaches to the stabilizer. The graph in Fig. 6 illustrates the relationship between the stabilizer position and the amount of force produced by the downspring.

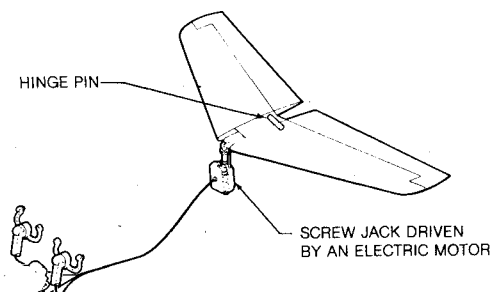


Fig. 4 Horizontal stabilizer trim system.

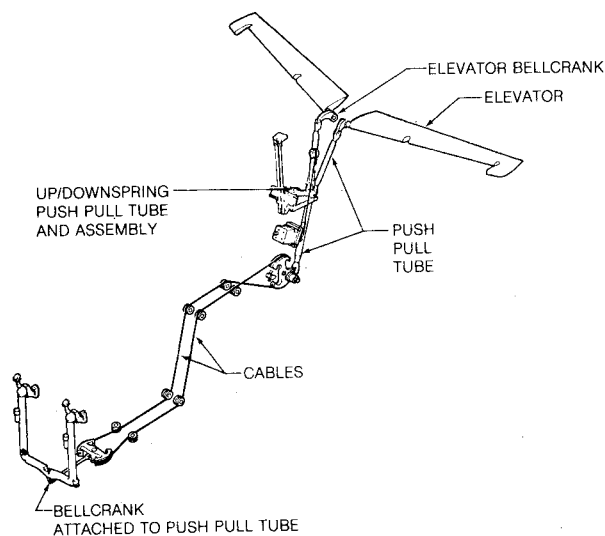


Fig. 5 Elevator control system.

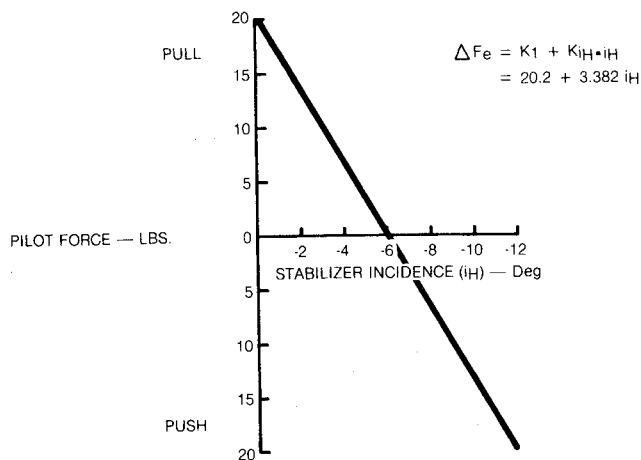


Fig. 6 Pilot force due to up/down spring.

Mathematical Modeling

Hinge Moment Equation

The relationship between the stabilizer position and the downspring force can be expressed mathematically as

$$\Delta F_e = K_l + K_{i_H} \cdot i_H \quad (1)$$

The measured stick force can be expressed as

$$F_{e_{\text{measured}}} = -G_e \cdot H_e + \Delta F_e \quad (2)$$

Substituting Eq. (1) into Eq. (2) and solving for hinge moment

$$H_e = \frac{F_{e_{\text{measured}}} - \Delta F_e}{-G_e} = \frac{F_{e_{\text{measured}}} - K_l - K_{i_H} \cdot i_H}{-G_e} \quad (3)$$

The hinge moment about the elevator hinge line can be expressed as

$$H_e = H_0 + H_\alpha \cdot \alpha_H + H_{\delta_e} \cdot \delta_e \quad (4)$$

where

$$\alpha_H = \alpha \left(1 - \frac{\partial \epsilon}{\partial \alpha} \right) - \epsilon_0 + i_H \quad (5)$$

Consequently, two hinge moment responses were available: one was determined directly from a Wheatstone bridge, measuring hinge moments about the hinge line; the other was computed using a strain gage which measures pilot input forces to the elevator control column. To take into account these two measurements, the following equation was used:

$$H_e = (1 - \lambda) H_{e_{\text{measured}}} + \lambda \left[\frac{F_{e_{\text{measured}}} - K_l - K_{i_H} \cdot i_H}{-G_e} \right] \quad (6)$$

The λ term can be used in one of two ways: either as a switch which would eliminate one or the other measurement, or to give more emphasis to the measurement considered to be more reliable. Equation (6) was programmed directly into the Taylor-Iliff computer program. The variables λ , K_l , K_{i_H} , and G_e were made inputs to be read by the program. Since the measurements for hinge moment and elevator stick force were strain gages, both were considered reliable. As a result, values for λ were chosen to be one and zero. This procedure provided two sets of hinge-moment derivatives. These derivatives were computed using hinge moment measurements and elevator stick force measurements, *independently*.

Actuator Equation

Figure 7 shows the relationship between the strain gage measurement of the actuator load and the airloads due to

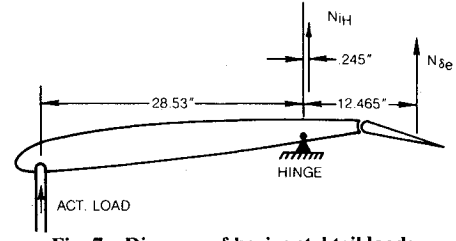


Fig. 7 Diagram of horizontal tail loads.

stabilizer incidence and those due to elevator deflection. The locations of the force vectors were determined using a doublet-lattice computer program. By summing the moments about the hinge point, the following equations can be derived.

$$\begin{aligned} \Sigma M_{\text{hinge}} &= 0.245 \cdot \overline{N_{iH}} \cdot \alpha_H \\ &+ 12.465 \cdot N_{\delta_e} \cdot \delta_e - 28.53 \cdot \text{ACTLOD} = 0 \\ \text{ACTLOD} &= 0.00859 \cdot N_{iH} \cdot \alpha_H + 0.4369 \cdot N_{\delta_e} \cdot \delta_e \end{aligned} \quad (7)$$

where α_H was defined in Eq. (5) and $N_{iH} = N$.

From Fig. 7, the normal airload due to stabilizer incidence, N_{iH} , is nearly on the hinge line. As a result, the likelihood of identifying the value of this derivative with any certainty is nil. Wind-tunnel values for this derivative were used for this equation since its value should not significantly affect the identification results of N . Good results, however, were expected of N_{δ_e} since this airload is much farther from the hinge.

Equations of State and Response

From Fig. 1, the equations of state and response in general form, can be written, respectively, as

$$\dot{x}(t) = Ax(t) + Bu(t)$$

$$y(t) = Fx(t) + Gu(t) + b$$

where $x(t)$ is the state vector of the position and velocity state variables, $u(t)$ is the control input vector, $y(t)$ is the resulting computed response vector, and b is the constant bias vector. For this investigation, the equation of state is:

$$\begin{bmatrix} \dot{q} \\ \dot{\theta} \\ \dot{\alpha} \end{bmatrix} = \begin{bmatrix} \overline{M_q} & 0 & M_\alpha \\ 1 & 0 & 0 \\ 1 & 0 & -N_\alpha \end{bmatrix} \begin{bmatrix} q \\ \theta \\ \alpha \end{bmatrix} + \begin{bmatrix} -N_{iH} \frac{WVI}{I_y g} & -\overline{N_{\delta_e}} \frac{WVI}{I_y g} & M_0 \\ 0 & 0 & 0 \\ -N_{iH} & -\overline{N_{\delta_e}} & -N_0 \end{bmatrix} \begin{bmatrix} i_H \\ \delta_e \\ 1 \end{bmatrix} \quad (8)$$

and the response equation is:

$$\begin{bmatrix} q \\ \theta \\ \alpha \\ a_n \\ \text{ACTLOD} \\ FE \\ H_e \end{bmatrix} = \begin{bmatrix} 1 & 0 & 0 \\ 0 & 1 & 0 \\ 0 & 0 & 1 \\ 0 & 0 & N_\alpha \frac{V}{g} \\ 0 & 0 & \overline{N_{iH}} \left(1 - \frac{\partial \epsilon}{\partial \alpha} \right) mV(0.00859) \\ 0 & 0 & 0 \\ 0 & 0 & H_\alpha \left(1 - \frac{\partial \epsilon}{\partial \alpha} \right) \end{bmatrix} \begin{bmatrix} q \\ \theta \\ \alpha \end{bmatrix} + \begin{bmatrix} 0 & 0 & 0 \\ 0 & 0 & 0 \\ 0 & 0 & 0 \\ N_{iH} \frac{V}{g} & \overline{N_{\delta_e}} \frac{V}{g} & N_{\delta_e} \\ N_{iH} mV(0.00859) & \overline{N_{\delta_e}} mV(0.4369) & N_{\delta_e} \\ 0 & FE_{\delta_e} & FE_0 \\ H_\alpha & H_{\delta_e} & -H_\alpha \epsilon_0 \end{bmatrix} \begin{bmatrix} i_H \\ \delta_e \\ 1 \end{bmatrix} + b \quad (9)$$

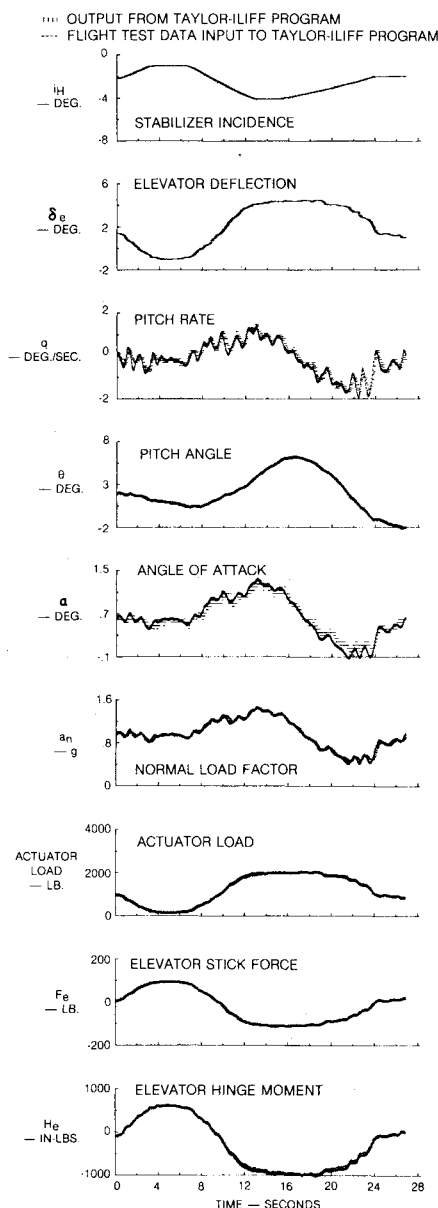


Fig. 8 Example time history of trim runaway.

During this study the observation was made, after some experience was gained, that not all of the derivatives shown in Eqs. (8) and (9) could be obtained. Reviewing the time histories shown in Fig. 8, the pilot corrected for the stabilizer trim runaways by using the elevator. As a result, these inputs tend to cancel out each other. Thus, either N_{iH} or $N_{\delta e}$ must be fixed in the equations. In the actuator load (ACTLOD) equation, Eq. (7), $N_{\delta e}$ was considered to be very accurate since strain gage measurements were involved. Thus, these values were fixed in the state equation and the normal acceleration response equation. Reasonable results were not possible for M_q . As shown in Fig. 8, pitching rate varies very little; consequently, M_q was fixed with analytical values. The downwash terms were fixed with wind-tunnel values.

These parameter identification computer programs contain an a priori option whereby values obtained from other sources can be input as starting values. These values also tend to force the answer to these starting values. In this study, a priori information was considered not available; consequently, this option was not used.

The normal airload derivatives in the actuator equation, Eq. (7), differs from the state equation, Eq. (8), by the factor mV . For example, in the state equation,

$$N_{\delta e} = C_{N_{\delta e}} (\bar{q}s/mV)$$

..... CASE 1 : FLIGHT TEST DATA INPUT TO MMLE PROGRAM.
 CASE 2 : OUTPUT TIME HISTORY FROM MMLE PROGRAM.

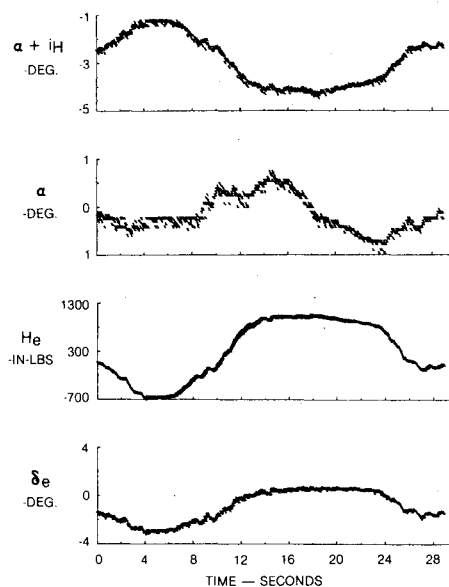


Fig. 9 Example of MMLE3 results for elevator hinge moment.

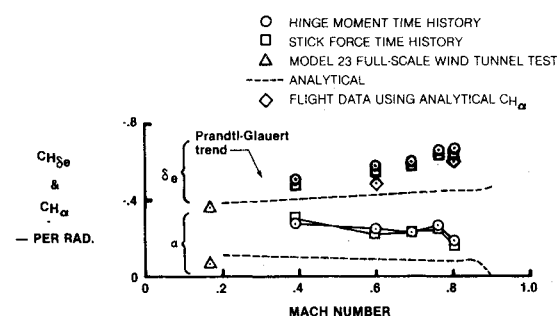


Fig. 10 Elevator hinge moment derivatives.

In the actuator equation,

$$N_{\delta e \text{ ACTLOD}} = C_{N_{\delta e}} \cdot \bar{q}s$$

Thus,

$$N_{\delta e \text{ ACTLOD}} = N_{\delta e} \cdot mV$$

Flight Conditions

The maneuver shown in Fig. 8 is a trim runaway condition required by the FAA in certifying an airplane. The maneuver is fairly static due to the pilot compensating for the runaway with elevator input. This made it difficult to separate the effects of the stabilizer and the elevator in the equations of state. The flight maneuvers were analyzed for air speeds ranging from Mach number 0.4 to 0.8. The airplane gross weights were approximately 15,000 lb at altitudes of 15,000 and 30,000 ft.

Time History Comparisons

Time history comparison plots are shown in Fig. 8 for the results from the Taylor-Iliff computer program. The comparisons from the Maine-Iliff program are very similar, and the parameter results were nearly identical.

Figure 9, using the Maine-Iliff program, illustrates results achieved for the hinge moment when not using a state equation. That is, all the time histories shown, except hinge moment, were used as inputs.

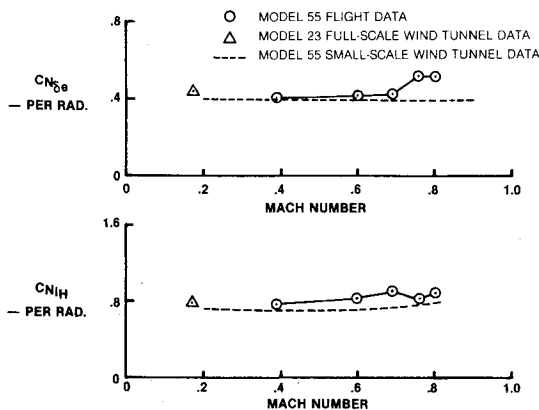


Fig. 11 Tail load derivatives.

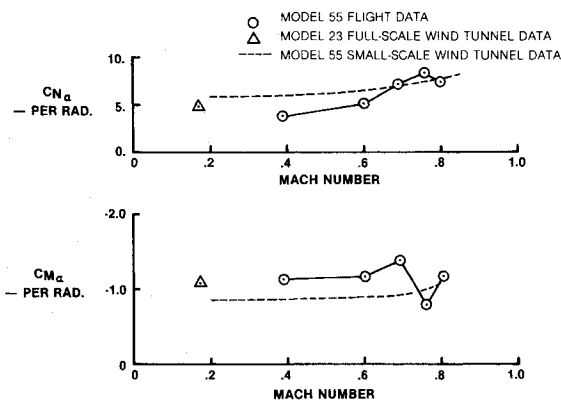


Fig. 12 Airplane derivatives due to angle of attack.

Identification Results

Figures 10-12 show the comparisons of the flight data results with full-scale model 23 and small-scale model 55 wind-tunnel test results. The parameters compared include $C_{H\delta_e}$, $C_{H\alpha}$, $C_{N\delta_e}$, $C_{N\delta_H}$, $C_{N\alpha}$, and $C_{M\alpha}$. The hinge moment curves also indicate the effect of using analytical results on the solution of $C_{H\delta_e}$.

Comparing the time histories of the two approaches indicated no difference. The tail derivatives show very good agreement with previous analyses. The airplane derivatives compare relatively well with full-scale wind-tunnel results, but show some disagreement with the small-scale wind-tunnel results.

The full-scale wind-tunnel test results are for a model 23 which now hangs in the National Air and Space Museum of the Smithsonian Institution in Washington, D.C. Model 23 is smaller than model 55; however, the horizontal tails are nearly identical. A bullet-shaped fairing at the top of the vertical fin no longer exists. These full-scale results are for reference purposes and should be judged on the basis of these differences.

Conclusions

The hinge moment derivative due to elevator deflection was shown to follow a Prandtl-Glauert Mach trend and agreed fairly well with full-scale wind-tunnel results at low speed. Considerable disagreement was noted for the hinge moment due to angle-of-attack derivative. Analytical values for this derivative reduced $C_{H\delta_e}$ somewhat. The time history comparisons of the two identification approaches provided nearly identical matches with flight data. The horizontal tail load derivatives provided very good correlation with previous analyses. The airplane derivative seemed to show better agreement with full-scale wind-tunnel results than with small-scale results.

The results of this study show that parameter identification techniques are valuable in determining horizontal tail load and hinge moment derivatives while determining airplane derivatives using the same flight records. Furthermore, these techniques enhance the certification process and provide confidence in the data used.

Acknowledgments

The authors wish to thank Larry Taylor, NASA Langley Research Center, Dr. Ken Iliff and Rich Maine, NASA Dryden Research Facility, for their guidance and support in using their computer programs.

References

- 1 Taylor, L.W. Jr. and Iliff, K.W., "Systems Identification Using a Modified Newton-Raphson Method—A FORTRAN Program," NASA TN D-6734, May 1972.
- 2 Maine, R.E. and Iliff, K.W., "User's Manual for MMLE3, a General FORTRAN Program for Maximum Likelihood Parameter Estimation," NASA TP-1563, Nov. 1980.
- 3 Maine, R.E., "Programmer's Manual for MMLE3, a General FORTRAN Program for Maximum Likelihood Parameter Estimation," NASA TP-1690, Aug. 1979.
- 4 Taylor, L.W. Jr. and Iliff, K.W., "A Modified Newton-Raphson Method for Determining Stability Derivatives from Flight Data," Presented at the Second International Conference on Computing Methods in Optimizing Problems, San Remo, Italy, Sept. 9-13, 1968.
- 5 Soderman, P.T. and Aiken T.N., "Full-Scale Wind Tunnel Tests of a Small Unpowered Jet Aircraft with a T-Tail," NASA TN D-6573, 1971.
- 6 Neal, R.D., "Correlation of Small-Scale and Full-Scale Wind Tunnel Data with Flight Test Data on the Learjet Model 23," SAE Paper 700237, March 1970.
- 7 Wingrove, R.C., "Review and Practical Aspects of Applying Aircraft Parameter Identification Techniques," Presented at AIAA First General Aviation Technologyfest, Nov. 1975.
- 8 Wingrove, R.C., "Estimation of Longitudinal Aerodynamic Coefficients and Comparison with Wind Tunnel Values," Parameter Estimation Techniques and Applications in Aircraft Flight Testing, NASA TN D-7647, 1974, pp. 125-147.
- 9 Park, G.D., "Parameter Identification Technology Used in Determining In-Flight Airload Parameters," *AIAA Journal of Aircraft*, Vol. 14, March 1977, pp. 251-256.
- 10 Park, G.D., "Determination of Tail-Off Aircraft Parameters Using Systems Identification," *Proceedings of the AIAA Third Atmospheric Flight Mechanics Conference*, June 1976, pp. 128-136.
- 11 Park, G.D. and Abal, M.H., "Determining Hinge Moments and Empennage Airload Parameters from Flight Data for Learjet Airplanes," *Proceedings of the Joint Automatic Control Conference*, Charlottesville, Va., Vol. 2, June 17-19, 1981.
- 12 Maine, R.E. and Iliff, K.W., "Maximum Likelihood Estimation of Translation Acceleration Derivatives from Flight Data," *Journal of Aircraft*, Vol. 16, Oct. 1979, pp. 674-679.
- 13 Taylor, L.W. Jr. and Iliff, K.W., "Determination of Stability Derivatives from Flight Data Using a Newton-Raphson Minimization Technique," NASA TN D-6579, 1972.
- 14 Taylor, L.W. Jr., Iliff, K.W., and Powers, B.G., "A Comparison of Newton-Raphson and Other Methods for Determining Stability Derivatives from Flight Data," Presented at AIAA Third Flight Test, Simulation and Support Conference, Houston, Tex., March 10-12, 1969.
- 15 Wolowicz, C.H., "Considerations in the Determination of Stability and Control Derivatives and Dynamic Characteristics from Flight Data," AGARD Rept. 549, Pt. 1, 1966.
- 16 Maine, R.E. and Iliff, K.W., "The Theory and Practice of Estimating the Accuracy of Dynamic Flight Derivatives Coefficients," NASA RP-1077, July 1981.
- 17 Iliff, K.W., "Aircraft Identification Experience," AGARD-LS-104, Paper 6, Athens, Greece, Nov. 1979.
- 18 Gilyard, G.B., "Flight-Determined Derivatives and Dynamic Characteristics of the CV-990 Airplane," NASA TN D-6777, May 1972.
- 19 Hamel, P.G., "Determination of Aircraft Dynamic Stability and Control Parameters from Flight Testing," *Dynamic Stability Parameters*, AGARD Lecture Series Preprint No. 114, March 1981, pp. 10-1—10-42.
- 20 *Parameter Estimation Techniques and Applications in Aircraft Flight Testing*, Symposium at the NASA Flight Research Center, April 24-25, 1973, NASA TN D-7647, 1974.

²¹ AGARD Conference Proceeding on Methods for Aircraft State and Parameter Identification, AGARD-CP-172, 1975.

²² Iliff, K.W., "Identification and Stochastic Control of an Aircraft Flying in Turbulence," *Journal of Guidance and Control*, Vol. 1, March-April 1978, pp. 101-108.

²³ Iliff, K.W. and Maine, R.E., "Observations of Maximum Likelihood Estimation of Aerodynamic Characteristics for Flight Data," *Journal of Guidance and Control*, May-June 1979, pp. 228-234.

²⁴ Maine, R.E. and Iliff, K.W., "Use of Cramer-Rao Bounds on Flight Data with Colored Residuals," *Journal of Guidance and Control*, March-April 1981, pp. 207-213.

²⁵ Maine, R.E. and Iliff, K.W., "Formulation and Implementation of a Practical Algorithm for Parameter Estimation with Process and Measurement Noise," *AIAA Atmospheric Flight Mechanics Conference*, Danvers, Mass., Aug. 11-13, 1980.

²⁶ Taylor, L.W. Jr., "Applications of Parameter Identification in the Study of Spinning Airplanes," AIAA Paper 82-1309, Jan. 1982.

²⁷ Pamadi, B.N. and Taylor, L.W., Jr., "An Estimation of Aerodynamic Forces and Moments on an Airplane Model Under Steady-State Spin Condition," AIAA Paper 82-1311, Jan. 1982.

²⁸ Wells, W.R. and Klein, V., "Parameter Estimation Applied to General Aviation Aircraft—A Case Study," AIAA Paper 82-1313, Jan. 1982.

²⁹ Wingrove, R.C. and Bach, R.E., "General Aviation Accidents Using ATC Radar Records," AIAA Paper 82-1310, Jan. 1982.

³⁰ Clark, R. and Roskam, J., "Simple, Low Cost Application of a Flight Test Parameter Identification System," AIAA Paper 82-1312, Jan. 1982.

³¹ Dwyer, J.P. and Tooley, E., "First Experience with Telemetry and Real Time Data Reduction at Gates Learjet," *Society of Flight Test Engineers Tenth Annual Symposium Proceedings*, Sept. 1979.

From the AIAA Progress in Astronautics and Aeronautics Series...

ENTRY HEATING AND THERMAL PROTECTION—v. 69

HEAT TRANSFER, THERMAL CONTROL, AND HEAT PIPES—v. 70

Edited by Walter B. Olstad, NASA Headquarters

The era of space exploration and utilization that we are witnessing today could not have become reality without a host of evolutionary and even revolutionary advances in many technical areas. Thermophysics is certainly no exception. In fact, the interdisciplinary field of thermophysics plays a significant role in the life cycle of all space missions from launch, through operation in the space environment, to entry into the atmosphere of Earth or one of Earth's planetary neighbors. Thermal control has been and remains a prime design concern for all spacecraft. Although many noteworthy advances in thermal control technology can be cited, such as advanced thermal coatings, louvered space radiators, low-temperature phase-change material packages, heat pipes and thermal diodes, and computational thermal analysis techniques, new and more challenging problems continue to arise. The prospects are for increased, not diminished, demands on the skill and ingenuity of the thermal control engineer and for continued advancement in those fundamental discipline areas upon which he relies. It is hoped that these volumes will be useful references for those working in these fields who may wish to bring themselves up-to-date in the applications to spacecraft and a guide and inspiration to those who, in the future, will be faced with new and, as yet, unknown design challenges.

Volume 69—361 pp., 6 × 9, illus., \$22.00 Mem., \$37.50 List
Volume 70—393 pp., 6 × 9, illus., \$22.00 Mem., \$37.50 List

TO ORDER WRITE: Publications Dept., AIAA, 1290 Avenue of the Americas, New York, N.Y. 10104